Radical scavenging and antioxidant properties of green zinc oxide nanoparticles from *Anacardium occidentale* leaves

AUTHORS:
Florence N. Nworah[1,2]
Nancy C. Igwebuike[2,3]
Ifeoma F. Chukwuma[1,2]
Chigozie P. Odo[1,3,4]
Ozoemena E. Eje[1,3,5]

AFFILIATIONS:
[1]Pharmacology Unit, Department of Biochemistry, University of Nigeria, Nsukka, Enugu State, Nigeria
[2]Department of Genetics and Biotechnology, University of Nigeria, Nsukka, Enugu State, Nigeria
[3]COVE-UP Analytical Laboratories, University of Nigeria, Nsukka, Enugu State, Nigeria
[4]Department of Chemistry and Biochemistry, University of South Carolina, Columbia, South Carolina, USA
[5]Department of Chemistry, Federal College of Education (Technical), Isu, Ebonyi State, Nigeria

CORRESPONDENCE TO:
Ozoemena Eje

EMAIL:
ozoemena.eje.pg01794@unn.edu.ng

DATES:
Received: 18 Sep. 2024
Revised: 11 Mar. 2025
Accepted: 13 May 2025
Published: 29 Sep. 2025

HOW TO CITE:
Nworah FN, Igwebuike NC, Chukwuma IF, Odo CP, Eje OE. Radical scavenging and antioxidant properties of green zinc oxide nanoparticles from *Anacardium occidentale* leaves. S Afr J Sci. 2025;121(9/10), Art. #20104. https://doi.org/10.17159/sajs.2025/20104

ARTICLE INCLUDES:
☒ Peer review
☐ Supplementary material

DATA AVAILABILITY:
☐ Open data set
☐ All data included
☒ On request from author(s)
☐ Not available
☐ Not applicable

EDITOR:
Philani Mashazi

KEYWORDS:
green synthesis, nanoparticles, characterisation, antioxidant, *Anacardium occidentale*

FUNDING:
None

Nanotechnology has become a focal point of interest on the road to disease intervention due to its vast applications in biomedicine and biotechnology. In this study, we evaluated the antioxidant properties of zinc oxide nanoparticles (ZnONPs) synthesised from *Anacardium occidentale* leaf extracts. The ZnONPs were characterised using UV-Visible and Fourier transform infrared (FTIR) spectroscopy, X-ray diffraction (XRD), scanning electron microscopy with energy dispersive X-ray (SEM-EDX), transmission electron microscopy (TEM) and gas chromatography-flame ionisation detection (GC-FID). Maximum UV-Vis spectra absorption revealed a prominent peak at 364–365 nm. The FTIR showed characteristic peaks at 3202 cm^{-1}, with the O-H functional vibration of carboxylic acids, and 1197 cm^{-1}, confirming the C-O stretch of alcohols. The absorption band of Zn tetrahedral coordination and Zn-O occurred at 869 cm^{-1} and 731–820 cm^{-1}, respectively. The ZnONPs particle size was 17.19 nm while SEM-EDX revealed the crystalline nature and elemental compositions of the ZnONPs. TEM showed particle size distribution to be within 10–29 nm, while GC-FID revealed the presence of flavonoids, alkaloids and polyphenolic compounds. ZnONPs exhibited high antioxidant properties using 2,2-diphenyl-1-picrylhydrazyl, 2,2′-azino-bis-(3-ethylbenzothiazoline-6-sulfonic, nitric oxide, thiobarbituric acid reactive substances, and ferric reducing antioxidant potential. Our findings show that *A. occidentale* leaves are a promising source of bioreductants for green synthesis, while the robust antioxidant properties exhibited by the ZnONPs are favourable in biomedical applications.

Significance:

This study shows a simple, cost-effective and eco-friendly approach for the synthesis of zinc oxide nanoparticles (ZnONPs) for therapeutic purposes. The utilisation of *Anacardium occidentale* leaves as a source of reducing agents for the capping and stabilisation processes makes it robust as plants are rich in bioactive compounds that possess a high therapeutic index. Antioxidant property assessment showed high scavenging activities for DPPH, ABTS and nitric oxide. Meanwhile, the ferric-reducing antioxidant power and the lipid peroxidation quenching properties exhibited by the ZnONPs would be favourable in controlling inflammation, with efficient permeation of the nanoparticles into targeted regions.

Introduction

The emergence of nanotechnology introduced a paradigm shift in tackling disease conditions from the use of conventional molecules and antibiotics with lower surface area. The drawbacks that accompany bulky drug agents in disease intervention, such as low permeability to body tissues and targeted organs, diffusion restriction, low surface area to volume ratio, and off-target delivery could be circumvented by the use of nanosize active agents. Nanoparticles are those materials with unique characteristic diameters in the range of 1–100 nm[1], although some nanomaterials or nanocomposites synthesised from biological polymers could have larger particle sizes up to 200 nm. Particles at the nanosize level exhibit unique properties due to increased surface area, a band gap of 3.3 eV, increased binding energy, and improved conduction resulting from an accumulation of higher surface energy and increased adherence. Therefore, nanomaterials have found applications in several fields and industries, such as the environment[2], agriculture, food, electronics, optics, biotechnology, biomedical, pharmaceuticals, wastewater treatment[3], optoelectronics, and antimicrobial agents[4].

Two major approaches – top-down and bottom-up – are used in nanoparticle synthesis. Nanoparticles can be organic or inorganic and are classified based on their dimensions that lie within the nanosize range. Organic nanoparticles include lipid nanoparticles (micelles, liposomes and nanocapsules), dendrimers, hybrids, nanospheres and compact polymerics.[5] Several metal oxide nanoparticles, including zinc oxide (ZnO), have been synthesised using chemical-based bottom-up strategies such as sol gelling, homogeneity-precipitation, organic-metal synthesis, spray pyrolysis, microwaving, and thermal evaporation, among others. However, these methods are hazardous, laborious, and expensive, thereby limiting their applications. This compelled the need to develop more efficient, environmentally friendly, non-toxic, and biocompatible strategies for the production of nanosized materials. ZnO is a promising and thermostable metallic oxide nanoparticle with broad applicability due to its unique antioxidant and anti-inflammatory properties. Besides optical, chemical sensing, semiconductor, electrical conductivity and piezoelectric properties, the mixture of ZnO nanoparticles (ZnONPs) and a chitosan hydrogel exhibits a high capacity for absorbing wound exudates, enables the production of haemostatic blood clots, and exhibits antimicrobial properties with no cytotoxicity. This surface modification and the intrinsic physicochemical properties of ZnONPs determine how hazardous or safe they could be.[6] Balaure et al.[7] found that a collagen wound dressing containing ZnONPs and 1% orange essential oil exhibited rapid wound closure, also inhibited bacterial growth, and had excellent biocompatibility both in vitro and in vivo.

Alternatively, green synthesis is an aspect of green chemistry that offers a promising and low-cost approach to manipulating and fabricating nanoparticles by utilising materials from plants, animals and microorganisms. Plants are mostly used in green synthesis because of their abundance of phytochemicals such as flavonoids and polyphenolic compounds that are used as therapeutics in the maintenance of health and treatment of ailments. Various parts of plants (stems, roots, fruits, seeds, calluses, peels, leaves and flowers) are utilised in biological approaches to synthesise metallic nanoparticles of diverse shapes and sizes.[8] During the synthesis of nanoparticles, these secondary metabolites are involved in the capping and stabilisation phase, and – through electrostatic interaction and conventional hydrogen bonding – the metal ion as the nucleus keeps initiating nucleation with other bioactive compounds, including carbohydrates and amino acids.[1] The exact modality of plant-mediated synthesis of nanomaterial is vague and not known because of the diverse nature of the phytochemical constituents of plant material. It has been reported that the antioxidant properties of polyphenolic bioactives make them suitable reductants, which also enhances the stability of nanoparticles during synthesis.[9]

The plant *Anacardium occidentale* (cashew) is found globally and belongs to the family Anacardiaceae (Figure 1). It is mostly grown in the Western parts of Africa, particularly in Dormaa Ahenkro in the Brong-Ahafo Region of Ghana and in Nigeria as a cash crop. *Anacardium occidentale* species have shown some ethnopharmacological benefits, especially in the treatment of several ailments due to their antidiabetic, anti-inflammatory, antibacterial, antifungal and antioxidant properties. Bioactive compounds from *A. occidentale* crude extracts possess a considerable therapeutic index in their bulky state; nevertheless, utilisation of this plant's leaves as a reducing agent source in the synthesis of metal-mediated nanoparticles could enhance their potential for use as efficient therapeutics. Different biological agents have been used to synthesise nanoparticles over the years; a variety of prokaryotes and eukaryotes are employed in the process of synthesis to create metallic nanoparticles[10], and viruses, fungi, algae and plants have also been used[11].

One of the widely used metallic nanoparticles that has garnered significant attention in the biomedical industries is zinc oxide nanoparticles due to their wide applications. Previous studies have demonstrated that ZnONPs synthesised from *Citrus sinensi*[12], *Justicia adhatoda*[13], *Lycopersicon esculentum*[14], *Chlamydomonas reinhardtii*[15], *Agathosma betulina*[16], *Arthrospira platensis*[17], *Moringa olifera*[18], *Ocin tenuiflorum*[19] and others have exhibited antioxidant properties both in vitro and in vivo and could be harnessed in the treatment of inflammation, cancer and infectious diseases, as well as in medical devices[16]. Synthesising nanosize biomolecules using bioactive compounds from *A. occidentale* leaf extracts would improve their efficacy in effective disease targeting. The biotechnological and applied microbiological uses of nanoparticles have grown as a result of their unique characteristics, such as large surface area, bioactivity, bioavailability, and bio-absorption.[20] In some fields of research – such as drug and gene delivery, cancer therapy, and imaging of cellular compartments – experts have referred to nanoparticles as a wonder of modern medicine. To the best of our knowledge, the different in vitro antioxidant models used in assessing the antioxidant properties of ZnONPs have not been reported in any work. In addition, the use of gas chromatography-flame ionisation detection (GC-FID) in elucidating the possible capping and stabilising bioactive compounds makes this study unique. We explored the synthesis and spectroscopic characterisation of ZnONPs from *A. occidentale* leaves and evaluated the antioxidant properties which would contribute to revolutionalising disease treatment in the field of nanomedicine globally.

Materials and methods

Collection of plant material

Fresh leaves of *Anacardium occidentale* were gathered on 10 March 2024 in Ezimo in the Udenu Local Government Area of Enugu State, Nigeria. The leaves were then air dried at room temperature and ground into a fine powder using a Corona Manual Heavy Metal Grinder.[21]

Chemicals and reagents

All the chemicals used for this experiment were pure and analytical grade. Zinc sulfate, sodium hydroxide, 2,2-diphenyl-1-picrylhydrazyl (DPPH), thiobarbituric acid (TBA), potassium bromide (KBr), acetic acid, iron sulfate ($FeSO_4$), methanol, 2,2'-azino-bis-ethylbenzothiazoline-6-sulfonic (ABTS) acid, sodium dodecyl sulfate (SDS) and trichloroacetic acid (TCA) are products of Sigma Aldrich (USA); sulfanilic acid, naphthyl ethylenediamine dihydrochloride, sodium nitroprusside, phosphomolybdic acid, sodium phosphate, ammonium molybdate, potassium ferric cyanide, ferric chloride and ammonium ferric sulfate were obtained from Molychem, India (British Drug House); ascorbic acid (AA) was obtained from Qualikems, India; and tetraoxosulfate (IV) acid (H_2SO_4) was obtained from Fluka, Germany.

Equipment and apparatus

All equipment used was obtained either from the Department of Biochemistry's laboratory unit at the University of Nigeria, Nsukka: electronic balance, spectrophotometer, temperature-controlled water bath, oven (BINDER Forced Air Circulation Oven, Germany); or *COVE-UP* Analytical Laboratories, University of Nigeria: centrifuge (Vickas Ltd,

Figure 1: *Anacardium occidentale* leaves

England), magnetic stirrer (LabTech MSH-200D Digital Magnetic Stirrer, Germany), spatula, conical flasks, beakers, magnetic bar. Nano Research Laboratories, University of Nigeria provided the UV3600-UV-vis-NIR Spectrophotometer; Ahmadu Bello University, Zaria, Nigeria provided the Nicolet 6700 FT-IR (Thermo Scientific; Oxford Inca Penta FeTX3 EDS instrument connected to Carl Zeiss EVO MA, Rigaku Mini-flex II system using nickel filtered CuKα radiation); and Springboard Laboratories, Awka, Anambra State, Nigeria provided the GC-FID (Alginate Technology).

Preparation of plant material

The hot-percolation approach, as described by Nduka et al.[22], was adopted to extract the bioactive compounds from the ground leaves. Briefly, 60 g of the ground leaves of *A. occidentale* was weighed into 1 L of deionised water and heated for 40 min at 100 °C with continuous stirring. Then, after cooling, the solid residues were separated via filtration through a cheesecloth to obtain the clear filtrate and further centrifuged at 5000 rpm for 10 min. The clearer top layer rich in bioactive compounds from the *A. occidentale* leaves was carefully decanted into a clean container for further use in the synthesis of ZnONPs.

A. occidentale *mediated synthesis of ZnONPs*

ZnONPs were synthesised from the prepared plant extracts using a slightly modified method adapted from Nduka et al.[22] The freshly prepared 100 mM $ZnSO_4$ solution was mixed with the plant extract in the ratio of 1:3 by slowly dropping the $ZnSO_4$ from a burette into a beaker containing the extract whilst stirring continuously with a magnetic stirrer. ZnONP formation was confirmed by a noticeable colour change in the solution, with the nanoparticles precipitating at the bottom of the flask. To purify the ZnONPs, the solution was centrifuged at 172.9 x g for 15 min using a low-speed centrifuge (Vickas Ltd, England). The resulting pellet was then re-dispersed in deionised water and dried in the oven at 50 °C for 24 h. The nanoparticles were stored in a container inside a desiccator containing silica gel to maintain stability and prevent moisture absorption.

Spectroscopic characterisation of A. occidentale *ZnONPs*

Ultraviolet-Visible spectroscopy

UV-Vis spectroscopy is a technique used to monitor the optimum conditions for forming ZnONPs by analysing the optical interaction of the particles through surface plasmon resonance. After 1:10 dilution of the crude extract of *A. occidentale* and $ZnSO_4$ solution, it was transferred into a quartz cuvette and subjected to a UV-VIS spectrophotometer within the wavelength range of 200–1100 nm. The energy band gap was estimated from the spectra.[22,23]

Fourier-transform infrared spectroscopy

The functional groups of the synthesised ZnONP were evaluated using a Fourier-transform infrared (FTIR) spectrometer (Nicolet 6700 FT-IR, Thermo Scientific) whose wavenumber ranged from 4000 cm^{-1} to 450 cm^{-1}. The sample for FTIR analysis was prepared by grinding the ZnONPs with a KBr pellet. The power "On" button of the instrument and the computer were turned on for 10–15 min to achieve system warm-up. Thereafter, the "MicroLabs PC window" and the "Start" circuits were closed to initiate the sampling operation, followed by the selection of the operation method of "Absorbance or transmittance". Before placing the samples, the organic solvent was used to clean the crystal and the "Next" icon was selected to check the crystal and collect the background reading. A 10 mg sample of *A. occidentale* ZnONP was placed on the crystal and pressed to form a pellet. Then, the alignment of the sample was checked to ensure proper sampling, the sample identity was coded, the "Next" button was clicked, then right-clicked to pick the peaks, and the peaks were selected and labelled, before "Run" was selected for analysis.

Scanning electron microscopy

The morphology and the elements present in the synthesised ZnONPs were evaluated using scanning electron microscopy coupled with energy dispersive X-ray spectroscopy (SEM-EDX). Briefly, *A. occidentale* ZnONPs were placed on a double adhesive sample stub and coated by a sputter coater (model Q150R, Quorum Technologies) with 5 nm of gold, taken to the chamber of the SEM machine and viewed through NaVCaM for focusing and adjustment.[24] It was then transferred to SEM mode and focused as the resolution was automatically adjusted. Thereafter, the structural appearance of different magnifications was captured and the EDX revealed the elements present.

X-ray diffraction spectroscopy

The crystallographic structures of the *A. occidentale* ZnONPs were analysed using X-ray spectroscopy. Briefly, *A. occidentale* ZnONPs were finely ground, homogenised, and compressed in a flat sample holder. Smooth adjustment for analysis was made by creating a smooth and flat surface on the ZnONP and mounting it on the X-ray diffraction (XRD) cabinet.[25] The XRD vibration and signal patterns were recorded using CuKα radiation with a wavelength (λ) of 1.5406 Armstrong, a voltage and current of 40 kV and 30 mA, respectively. The 2θ angular range spanned from 4° to 75°, with a step size of 0.026261° and a counting time of 8.67 seconds per step. The intensity of diffracted light was recorded as the ratio of the peak intensity to the highest peak (relative intensity = I/I1 x 100). Particle size was estimated using Scherer's formula (Equation 1):

$$\text{Particle size (nm)} = \frac{K\lambda}{\beta Cos\theta} \qquad \text{Equation 1}$$

where K = shape factor = 0.95, λ = CuKα with a wavelength of 1.5406 Å (0.154 nm), θ = Bragg's angle of diffraction in radians and β = full width at half maximum of the diffraction peak.

Transmission electron microscopy

The size and shape of the phytosynthesised ZnONPs were determined by transmission electron microscopy (TEM). The TEM images were obtained using a Philips Tecnai10 transmission electron microscope. Before analysis, ZnONPs were sonicated for 5 min, and a drop of appropriately diluted sample was placed onto a carbon-coated copper grid. The electron micrographs were used to investigate the surface features of the phytosynthesised ZnONPs.[26,27] The unique morphology of the microwave-generated ZnONPs and the particle size distributions were visualised from the TEM images.

GC-FID and phytochemical analysis of A. occidentale *ZnONPs*

To ascertain the bioactive and phytochemical compounds involved in the capping process for the synthesis of ZnONPs from *A. occidentale,* the ZnONP extract was washed three times with 10 mL of 10% v/v ethanol aqueous solution. The solution was dried using anhydrous sodium sulfate and the solvent was evaporated. The sample was solubilised in 1000 uL of pyridine, of which 200 uL was transferred to a vial for analysis. The phytochemical analysis was performed using a Buck M910 gas chromatograph equipped with a flame ionisation detector. A syringe was used to draw 0.1 mL of the extract and inject it into the gas chromatograph. The sample is separated in the GC column as each analyte passes through the flame, fuelled by hydrogen and zero air, which ionises the carbon atoms and detects the bioactive compounds.[28]

Evaluation of antioxidant properties of A. occidentale *ZnONPs*

Lipid peroxidation inhibition

The potential for lipid peroxidation inhibition of *A. occidentale* ZnONP was evaluated through the presence of thiobarbituric acid reactive substances (TBARs), as described by Ohkowa et al.[29] Different concentrations of *A. occidentale* ZnONPs (1.39–12.5 mg/mL) were prepared and 500 μL of 10% v/v egg yolk and 50 μL of a 70 mM solution of $FeSO_4$ were added to induce peroxidation of lipids. A 1.5 mL solution of 20% acetic acid, 1.5 mL of 0.8% TBA in 1.1% SDS, and 50 μL of 20% TCA were added and the solution was vigorously shaken for proper mixing and heated at 95 °C for 1 h after incubation for 30 min at room temperature. The absorbance

was recorded using a spectrophotometer at 532 nm against the blank. The level of peroxidation quench was evaluated using Equation 2:

$$\frac{C-E}{C} \times 100 \quad \text{Equation 2}$$

where C is the control (without extract) and E represents (Abs_{532}+TBA - Abs_{532}-TBA).

Estimation of DPPH radical scavenging activity

Different concentrations of *A. occidentale* ZnONPs were pipetted into test tubes as described above and 1.5 mL of methanolic 0.18 mM DPPH solution was added and thoroughly mixed. The samples were then taken into a dark cupboard for 30 min and the absorbances were read at 517 nm against the blank.[30] The DPPH radical scavenging property was calculated using Equation 3:

$$\textit{Radical scavenging}\ (\%) = \frac{A_{517\ blank} - A_{517\ treatment}}{A_{517\ treatment}} \times 100 \quad \text{Equation 3}$$

Determination of ABTS* radical scavenging property

The ABTS* radical scavenging property was ascertained as described by Pejin and Bogdanović-Pristov[31] with slight modification. Different concentrations of *A. occidentale* ZnONPs, as described above, were taken into test tubes. The ABTS* radical was produced by the addition of potassium persulfate and allowed to stand for 24 h in the dark. Then 1 mL of the radical solution was added to varying concentrations of the ZnONPs, and allowed to stand in the dark for 30 min. Absorbance was recorded at 730 nm using a spectrophotometer (Spectrumlab $23_{A,}$ England) at room temperature. The percentage scavenging activity was estimated, as in the case of DPPH.

Evaluation of nitric oxide scavenging

Nitric oxide scavenging activity (NOSA) was evaluated as outlined by Jagetia and Baliga[32]. Briefly, nitric oxide (NO) was generated using 2 mL of 10 mM aqueous solution of sodium nitroprusside at physiological pH. Varying concentrations of *A. occidentale* ZnONPs were then pipetted into the test tubes. After 150 min, 0.5 mL of Griess solution was added and the samples were left to stand for 30 min, after which absorbance was measured at 540 nm.

Determination of ferric-reducing power

The ability to reduce ferric ions to ferrous ions was evaluated by adding 1 mL of 1.0% potassium ferric cyanide into a test tube containing 0.5 mL of 0.1 M sodium phosphate buffer (pH 6.6) and 1 mL of 0.5% TCA and centrifuging at 4000 rpm after incubation at 50 °C for 20 min. The supernatant was diluted with an equivalent volume of distilled water, 0.1 mL of freshly prepared ferric chloride was added, and the absorbance read was at 700 nm against the blank.[33]

Statistical analyses

Statistical Package for Social Sciences (SPSS) version 23 was used to obtain the descriptive statistics, and the IC_{50} values were calculated from the dose-response curve using Origin Pro 2024b software.

Results and discussion

UV-Vis spectroscopy of A. occidentale *ZnONPs*

The first sign of a successful ZnONP synthesis was the brown precipitate that appeared when the plant extract was added to zinc sulfate. The UV-Vis spectra revealed a pronounced absorption peak around 364–365 nm. Notably, the ZnONP, NaOH-assisted ZnONP, and the extract demonstrated peak absorption at a wavelength of 365 nm, with abundance (a.u) values of 3.313, 2.038 and 0.745, respectively, confirming the effective synthesis of ZnONPs using the aqueous extract of *A. occidentale*. In contrast, the zinc sulfate solution exhibited its maximum absorption at 364 nm, with a value of 1.264. The surface plasmon resonance of the synthesised NPs is responsible for the solution's gradual change in colour. The primary cause of the bioreduction of Zn^{2+} to Zn^{0} could be the phytochemicals found in *A. occidentale* leaf extracts.[34] In this study, there was a progressive surface plasmon resonance band appearance between 370 nm and 400 nm, indicating ZnONP formation (Figure 2), while the absorbance peak at 380 nm was the maximum value. Sharmila et al.[35] published similar results with an absorption peak for ZnONPs of 380 nm. This could be attributed to the presence of phytochemicals such as proteins, alkaloids, flavonoids and phenolics found in the *A. occidentale* leaf extract which functioned as biological reductants and are important in the formation of ZnONPs.[36] Similar findings were reported for seaweed extract and Madar latex ZnONPs which showed maximum absorption at 365 nm and 368 nm, respectively.[36] Additionally, ZnONPs produced from zinc acetate, zinc sulfate and zinc nitrate exhibited characteristic peaks at 334 nm, 338 nm and 361 nm, respectively, with decreased absorbance values.[10] Sutradha and Saha[37]

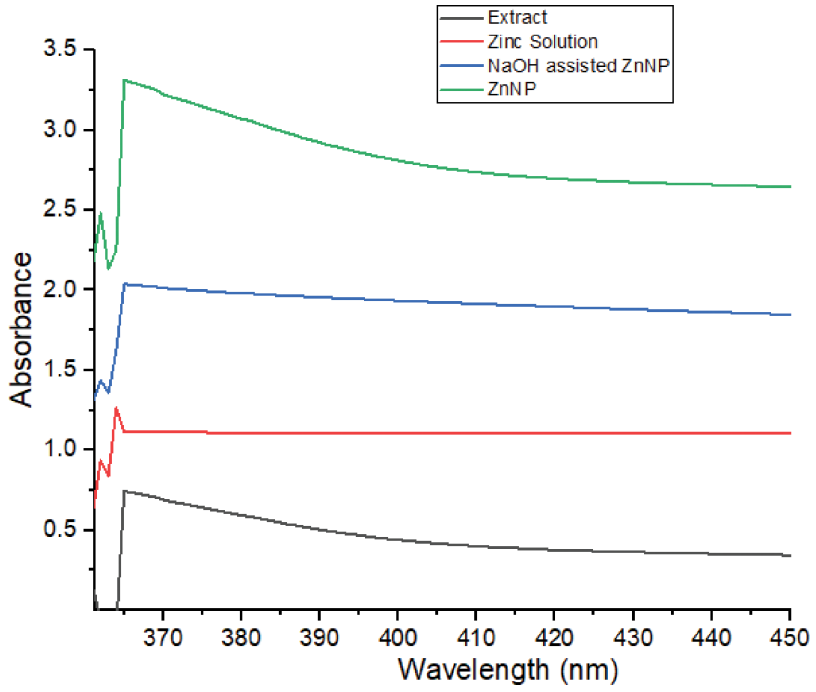

Figure 2: Ultraviolet spectra of the extract, zinc solution and zinc oxide nanoparticles (ZnNPs).

found that green-synthesised ZnONPs from tomato (*Lycopersicon esculentum*) displayed absorption peaks at 322 nm and 334 nm in UV-Vis spectral analysis. ZnONPs synthesised using seaweed absorbed light maximally at 384 nm; however, 373 nm was where the bulky zinc oxide absorbed what could be attributed to a wider energy band gap.[38]

The functional group identification of the stabilising reductants involved in the synthesis of ZnONPs was analysed using FTIR spectroscopy.[39,40] The distinctive peak vibration at 3201 cm^{-1} is an O-H bond with phenol and alcohol functional groups. The peak at 2113 cm^{-1} represents a —C≡C— stretch with alkynes as a functional group. Also, the vibrational peaks at 1602 cm^{-1} depict an N—H bond which shows the presence of a primary amine group due to the presence of peptide moieties from the leaf of *A. occidentale* (Figure 3). An N—O asymmetric stretch indicates the nitro compounds group at 1520 cm^{-1} and a 1442 cm^{-1} vibration reveals a C—C stretch (in-ring) which belongs to the aromatic group. The peak 1319 cm^{-1} represents a C—O stretch showing the presence of functional groups like alcohols, carboxylic acids, esters and ethers. The vibrational peaks 1088 cm^{-1} and 1025 cm^{-1} fit the C—N stretch attributed to the characteristic functional group of aliphatic amines. The peak 868 cm^{-1} represents the C—H "oop" of the aromatic and Zn-O bonding functional group. Moreover, 820 cm^{-1} and 730 cm^{-1} correspond to the C—Cl stretch and the alkyl halides functional group and Zn. The phenolic and the amide vibrations of phytocompounds (alkaloids, flavonoids and phenolics) and proteins could be responsible for nanoparticle stabilisation after capping.[41] Rao and Gautam[15] synthesised ZnO nanoflowers using *Chlamydomonas reinhardtii* and observed a peak at 3437 cm^{-1} due to O-H vibration, with shifts in the amide I and II peaks indicating ZnO nanoflower formation. Similarly, ZnONPs synthesised using *Malus pumila* showed peaks at 1018 cm^{-1} due to C-O stretching of amino acids, and peaks at 528, 475 and 429 cm^{-1} due to the hexagonal phase of ZnONPs.[42] For *Juglans regia* mediated ZnONPs, peaks at 575, 468 and 435 cm^{-1} were attributed to the hexagonal phase of ZnONPs.[42,43]

The EDX analysis revealed the elemental compositions with atomic and weight concentrations: carbon (87.20% and 79.59%), nitrogen (9.03% and 9.61%), zinc (1.08% and 5.37%), sodium (1.39% and 2.42%), sulfur (0.48% and 1.16%), aluminium (0.25% and 0.51%), potassium (0.12% and 0.36%), magnesium (0.17% and 0.32%), phosphorus (0.11% and 0.27%), silicon (0.12% and 0.25%) and chlorine (0.05% and 0.14%) (Table 1 and Figure 4). The variations of these elements may be attributed to possible compositions of *A. occidentale* which were also involved in the capping and stabilisation stage during nanoparticle formation.[44] Hence, zinc appeared to be in lower abundance compared to carbon due to the presence of phytocompounds that were involved in the reduction of Zn^{2+} to Zn^{0}. Similar outcomes were attained when ZnONPs were synthesised using seaweed, and EDX imaging revealed a pure form of the nanoparticle.[43] The EDX analysis of phytosynthesised ZnONPs from *Malus pumila* extract showed the main components as zinc (60.5%), oxygen (33.04%) and carbon (6.46%), whereas *Juglans regia* derived ZnONPs contained zinc (22.27%), oxygen (61.66%) and carbon (16.07%).[42] The SEM image of the nanoparticle shows the semi-crystalline nature of the ZnONPs at three magnifications: x 500, x 1000 and x 2000 (Figure 5).

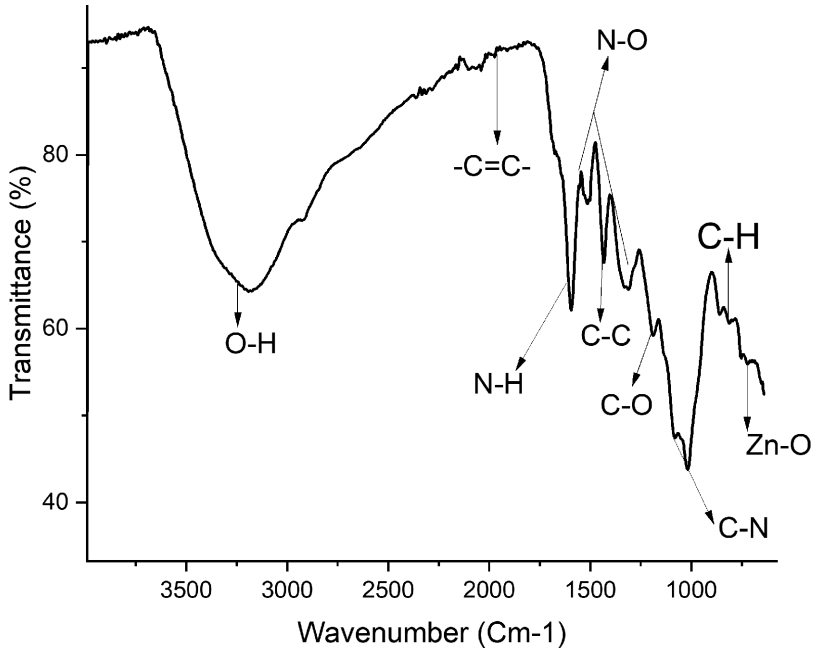

Figure 3: Fourier-transform infrared spectrum of *Anacardium occidentale* zinc oxide nanoparticles.

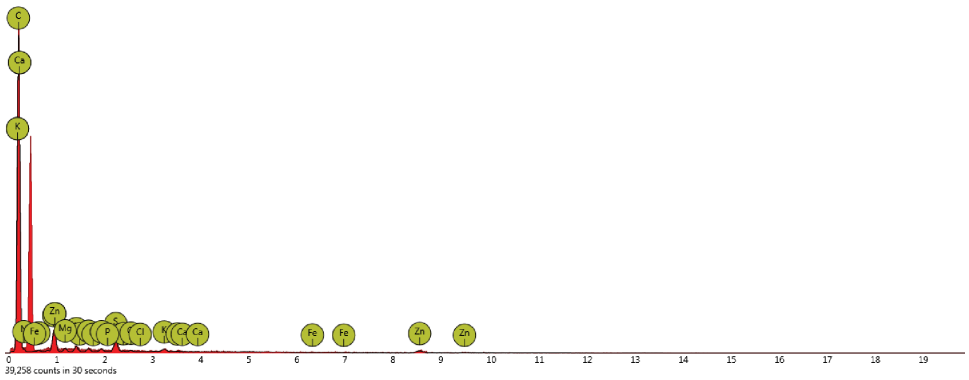

Figure 4: The energy dispersive X-ray spectrum of zinc oxide nanoparticles.

Table 1: Energy dispersive X-ray elemental analysis of zinc oxide nanoparticles

Element number	Element symbol	Element name	Atomic concentration (%)	Weight concentration (%)
6	C	Carbon	87.20	79.59
7	N	Nitrogen	9.03	9.61
30	Zn	Zinc	1.08	5.37
11	Na	Sodium	1.39	2.42
16	S	Sulfur	0.48	1.16
13	Al	Aluminium	0.25	0.51
19	K	Potassium	0.12	0.36
12	Mg	Magnesium	0.17	0.32
15	P	Phosphorus	0.11	0.27
14	Si	Silicon	0.12	0.25
17	Cl	Chlorine	0.05	0.14
20	Ca	Calcium	0.00	0.00
26	Fe	Iron	0.00	0.00

X-ray diffraction analysis, displayed in Figure 6, revealed peaks at 2θ values of 18.78, 20.58, 21.88, 26.34, 29.26, 33.94, 35.78, 38.02, 39.7, 41.24, 44.22, 53.0, 64.54 and 68.87°, matching the characteristic peaks of pure ZnO and confirming its semi-crystalline nature (Figure 6). Using Debye–Scherrer's formula, the average particle size was calculated to be 17.19 nm, while the individual particle sizes are represented in a histogram (Figure 7). Additionally, the average Bragg angle and the full width at half maximum were found to be 38.38° and 0.508, respectively. This is in agreement with the XRD pattern reported by Kumar et al.[45] Similar research on ZnONPs from *Citrus sinensis* found average crystal sizes of 24.3, 22.6 and 12.7 nm for different extract concentrations.[9] Rao and Gautam[15] described the X-ray diffraction pattern of ZnONPs as having a hexagonal wurtzite structure with lattice constants a = 3.239 Å and c = 5.203 Å, which were in agreement with the standard. Various Bragg reflections at 31.78° (100), 34.48° (002), 36.38° (101), 47.78° (102), 56.58° (110), 62.98° (103), 68.08° (112) and 69.18° (201) were observed. The average crystallite size was 21 nm, slightly higher than that reported in the present study. Similar results were observed during the synthesis of ZnONPs using seaweed extract and Madar latex, with particles being spherical and 40 nm in size.[41] The crystallite sizes of ZnONPs synthesised using *Malus pumila* and *Juglans regia* extracts were reported to be 46.41 nm and 90.80 nm, respectively.[42] The TEM analysis showed predominantly monodispersed spherical shapes ranging in size from 20 nm to 100 nm; the mean particle sizes at 20, 50 and 100 nm magnifications were 18.256, 17.977 and 17.999 nm, while the overall and average particle size was 18.07 nm (Figure 8) which coincided with the XRD value. The GC-FID analysis of the ZnONPs showed the presence of flavonoids (flavone, epicatechin, tangeretein, hesperidin, butein, apigenin, myricetin, naringenin and daidzein), polyphenolics (ellagic acid and vanillic acid) and alkaloids (lunamarin) (Table 2). These bioactive compounds participated in the capping and stabilisation of the synthesised nanoparticles.[21]

Antioxidant properties of A. occidentale *ZnONPs*

The antioxidant activity of the green-synthesised ZnONPs was evaluated using different models – TBARS, DPPH, NOSA and ABTS – as summarised in Table 3. The TBARS were analysed to ascertain the lipid peroxidation inhibitory properties of *A. occidentale* ZnONPs. When inhibition occurs, the decrease in the level of malondialdehyde formation is diagnostic for

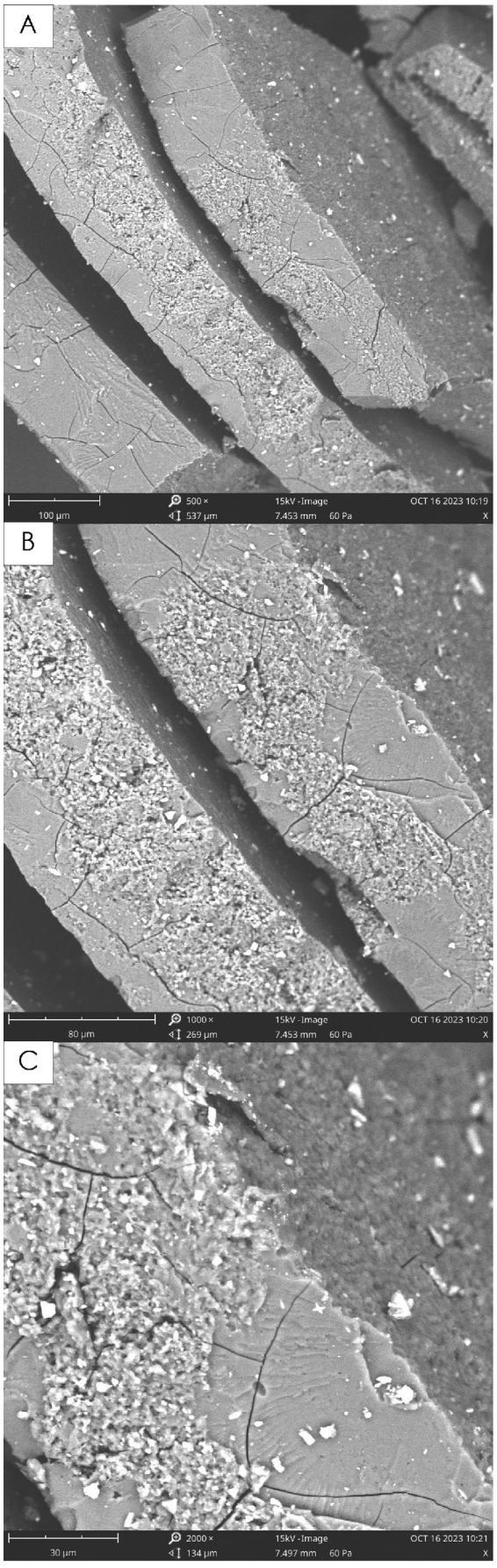

Figure 5: Scanning electron micrographs of *Anacardium occidentale* zinc oxide nanoparticles at three magnifications: (A) x 500, (B) x 1000 and (C) x 2000.

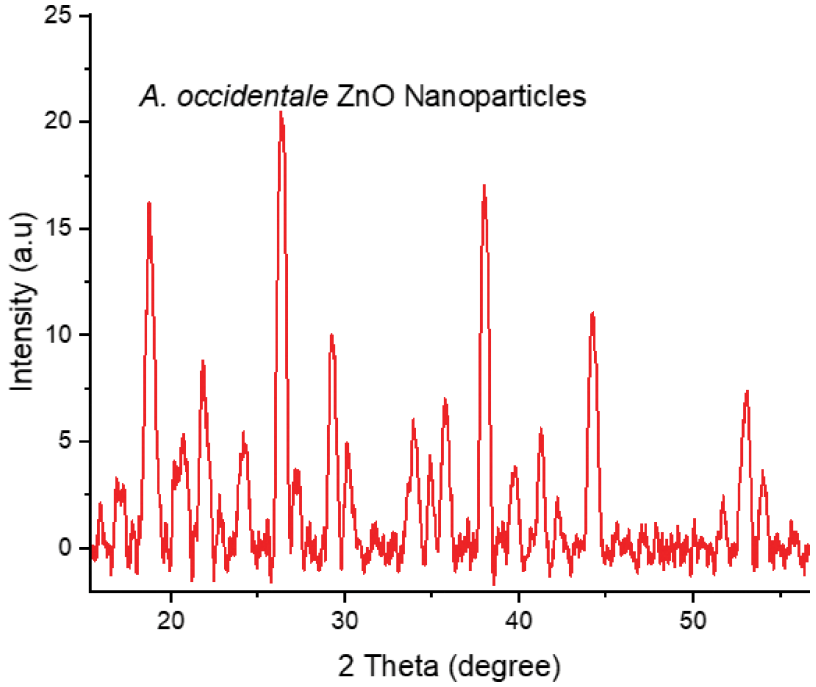

Figure 6: X-ray diffractogram of *Anacardium occidentale* zinc oxide nanoparticles.

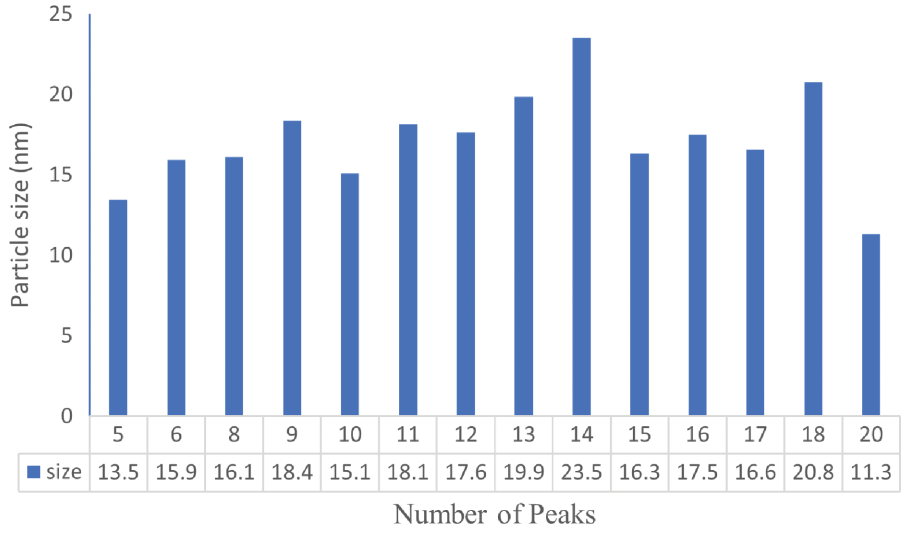

Figure 7: The individual peak particle sizes of *Anacardium occidentale* zinc oxide nanoparticles.

antioxidant and lipid peroxidation inhibition.[29] This study revealed that *A.occidentale* ZnONPs exhibited the highest inhibitory potential at 3.13 mg/mL; the IC_{50} value (the concentration of *A. occidentale* ZnONPs needed to cause 50% peroxidation) was 5.84 mg/mL. In terms of scavenging of the stable free radical, DPPH, the nanoparticles achieved 86.07 ± 2.4% scavenging of free radicals via abstraction of electron(s) from the gigantic ring of the toxic compound, with an IC_{50} value of 2.0 mg/mL. This cleavage of the structure ameliorates the toxicity of the radical through the collapsing of its structure, which was qualitatively indicated by the colour change from purple to yellow by the product of diphenylpicrylhydrazine due to its hydrogen-donating ability forming a stable diamagnetic molecule.[46] These pronounced antioxidative properties could be due to the wide range of phytochemical content (e.g. phenolics, alkaloids, flavonoids, tannins, saponins and terpenoids) in *A. occidentale* leaf extracts, which were involved as both stabilisation and capping agents during the synthesis of ZnONPs. Similar results were reported by Sharmila et al.[35] for ZnONPs mediated by plant extracts. ABTS*+ radical scavenging activities of *A. occidentale* ZnONPs rely on quenching the stable coloured radicals, which shows how efficient radical scavenging occurs.[47] The concentrations of 3.13 mg/mL and 12.50 mg/mL exhibited absolute (100%) scavenging properties, with an IC_{50} value of 0.75 mg/mL. The percentage of inhibition of nitrite (NO*) mopping up was decreased with increased ZnONP concentration as the maximum percentage was 70.20 ± 1.1% and the IC_{50} was 2.80 mg/mL. Hydrogen and electron-withdrawing or donating bioactive compounds would contribute to the competition with oxygen, thereby decreasing the production of nitrite ions.[48] It has been reported that ZnONPs enhance antioxidant activity to mop up free radicals and prevent the incidence of oxidative and nitrosative stress.[46-49] Other in vitro models used for antioxidant assessment of the ZnONPs was ferric-reducing antioxidant potential, which occurred in a concentration-dependent manner with 4.31–4.72 mg/g AAE compared to 0.54–0.83 mg/g AA (Figure 9). The deeper the bluish colouration as a result of antioxidants' electron donation at low pH, the greater the conversion of ferric ions to utilisable ferrous ions.[47,50,51]

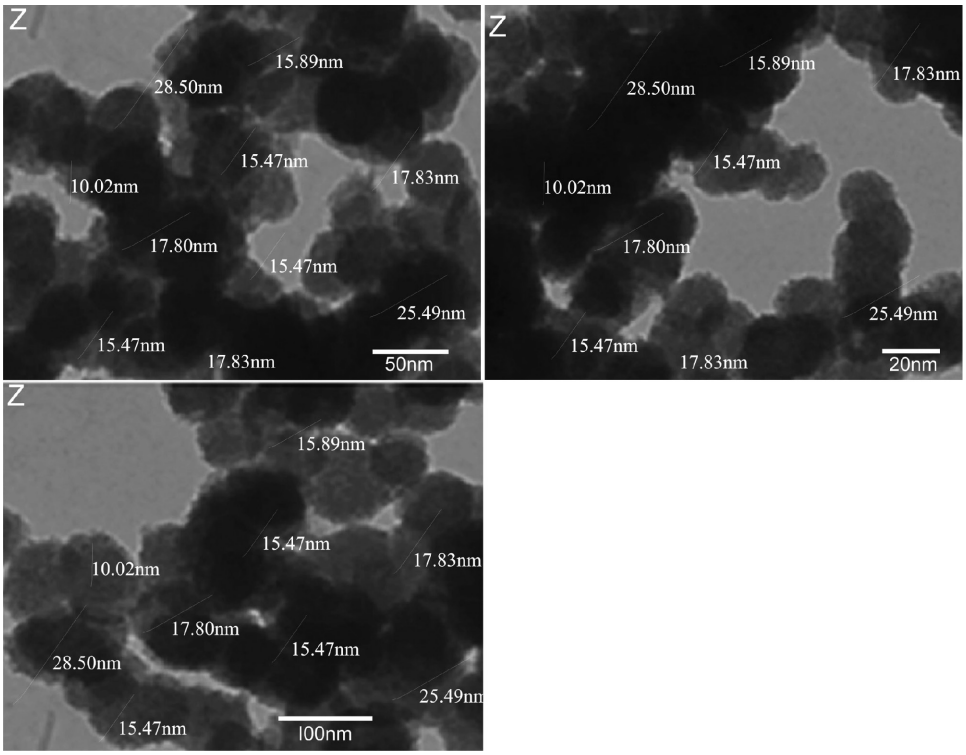

Figure 8: Transmission electron microscopy images of *Anacardium occidentale* zinc oxide nanoparticles.

Table 2: Summary of gas chromatography–flame ionisation detector analysis of zinc oxide nanoparticles

Retention time (min)	Area (pA*s)	Amount/area	Amount (ppm)	Common name	Molecular formula
7.107	1.00666	1.31970e-1	1.32849e-1	Artemetin	$C_{20}H_{20}O_8$
7.521	1.68323	1.34067e-1	2.25665e-1	Reveratrol	$C_{14}H_{12}O_3$
7.547	1.51709	1.34157e-1	2.03529e-1	Flavone	$C_{15}H_{10}O_2$
7.831	3.91197	1.37861e-1	5.39308e-1	Lunamarin	$C_{18}H_{15}NO_4$
8.494	3.30945	1.37302e-1	4.54393e-1	Nobeletin	$C_{21}H_{22}O_8$
8.645	1.54330	1.34627e-1	2.07769e-1	Ellagic acid	$C_{14}H_6O_8$
8.982	3.45640	1.37655e-1	4.75790e-1	Epicatechin	$C_{15}H_{14}O_6$
9.271	2.09336	1.35745e-1	2.84164e-1	Tangeretein	$C_{20}H_{20}O_7$
9.828	5.99481	1.39053e-1	8.33599e-1	Vanillic	$C_8H_8O_4$
10.132	3.18414	1.37666e-1	4.38349e-1	Hesperidin	$C_{28}H_{34}O_{15}$
10.214	7.02384	1.39100e-1	9.77018e-1	Butein	$C_{15}H_{12}O_5$
10.375	5.20451	1.36543e-1	7.10639e-1	Apigenin	$C_{15}H_{10}O_5$
11.551	3.95972	1.38091e-1	5.46802e-1	Myricetin	$C_{15}H_{10}O_8$
12.381	4.87746	1.38859e-1	6.77277e-1	Daidzin	$C_{21}H_{20}O_9$
12.525	2.17759	1.36376e-1	2.96971e-1	Isorhamnetin	$C_{16}H_{12}O_7$
12.629	3.60948	1.38037e-1	4.98242e-1	Naringenin	$C_{15}H_{12}O_5$
13.094	5.14517	1.38672e-1	7.13494e-1	Maricetin	$C_{20}H_{14}O_4$
14.109	15.40274	1.39952e-1	2.15565	Daidzein	$C_{15}H_{10}O_4$

Table 3: Antioxidant properties (%) of *Anacardium occidentale* zinc oxide nanoparticles

Concentration (mg/mL)	TBARS	DPPH	ABTS	NOSA
1.39	44.04 ± 2.3	81.22 ± 1.9	99.70 ± 1.3	70.20 ± 1.1
3.13	46.66 ± 1.4	86.07 ± 2.4	100.0 ± 0.8	58.03 ± 1.5
5.36	38.10 ± 3.1	69.17 ± 1.6	99.28 ± 1.5	29.49 ± 0.6
8.33	45.00 ± 2.1	65.73 ± 3.0	99.45 ± 0.3	16.69 ± 0.2
12.50	36.04 ± 2.5	63.85 ± 1.9	100.0 ± 0.3	8.11 ± 2.4
IC_{50}	2.14	2.00	0.75	2.80

Results are presented as mean ± SD of three determinations, n = *3*

TBARS = thiobarbituric acid reactive substances; DPPH = 2, 2-diphenyl-1-picrylhydrazyl; ABTS = 2, 2'-azino-bis-ethylbenzothiazoline-6-sulfonic (ABTS) acid; NOSA = nitric oxide scavenging activity

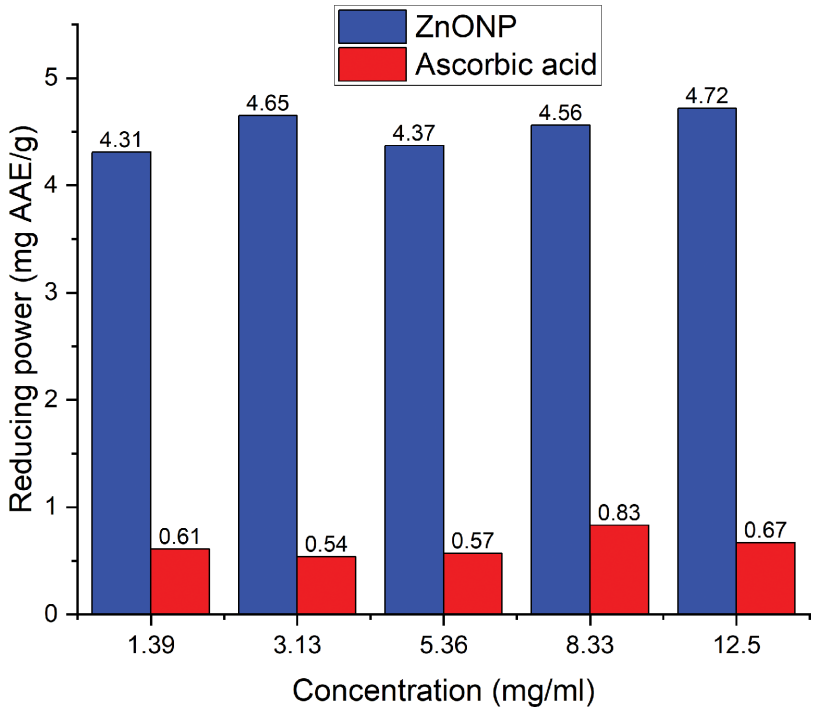

Figure 9: Ferric-reducing antioxidant power of zinc oxide nanoparticles (ZnONPs).

In conclusion, the results of this study reveal that ZnONPs synthesised from *A. occidentale* leaf extracts show excellent antioxidant properties using an in vitro model of ferric-reducing antioxidant power. The nanoparticles also showed free radical scavenging properties on DPPH, ABTS, NOSA and lipid peroxidation inhibition (TBARS). ZnONP formation was confirmed using UV-Vis spectroscopic absorption at 364–365 nm. The functional groups, morphology-elemental compositions and particle size(s) were analysed using FTIR, SEM-EDX, XRD and TEM spectroscopic techniques. Based on the antioxidant activities exhibited, ZnONPs could be harnessed for biomedical applications. Moreover, the green synthesis process is economical in terms of energy, time and simplicity and achieves high yields, making it suitable for large-scale production of nano-crystalline zinc oxide.

Data availability

The data supporting the results of this study are available upon request to the corresponding author.

Declarations

We have no competing interests to declare. We have no AI or LLM use to declare.

Authors' contributions

F.N.N.: Conceptualisation, supervision, resources, validation, writing – review and editing. N.C.I.: Investigation, formal analysis, writing – original draft. I.F.C.: Data curation, formal analysis, validation, writing – review and editing. C.P.O.: Conceptualisation, data curation, validation, writing – review and editing. O.E.E.: Conceptualisation, methodology, project management, investigation, data curation, writing – original draft, validation, formal analysis, writing – review and editing. All authors read and approved the final version.

References

1. Essien ER, Atasie VN, Nwude DO, Adekolurejo E, Owoeye FT. Characterisation of ZnO nanoparticles prepared using aqueous leaf extracts of *Chromolaena odorata* (L.) and *Manihot esculenta* (Crantz). S Afr J Sci. 2022;118(1–2), Art. #11225. https://doi.org/10.17159/sajs.2022/11225
2. Chen J, Guo Y, Zhang X, Liu J, Gong P, Su Z, et al. Emerging nanoparticles in food: Sources, application, and safety. J Agric Food Chem. 2023;71(8):3564–3582. https://doi.org/10.1021/acs.jafc.2c06740
3. Zahra Z, Habib Z, Chung S, Badshah MA. Exposure route of TiO_2 NPs from industrial applications to wastewater treatment and their impacts on the agro-environment. Nanomaterials. 2020;10(8), Art. #1469. https://doi.org/10.3390/nano10081469

4. Islam F, Shohag S, Uddin MJ, Islam MR, Nafady MH, Akter A, et al. Exploring the journey of zinc oxide nanoparticles (ZnO-NPs) toward biomedical applications. Materials. 2022;15(6), Art. #2160. https://doi.org/10.3390/ma15062160

5. Ojo OA, Olayide II, Akalabu MC, Ajiboye BO, Ojo AB, Oyinloye BE, et al. Nanoparticles and their biomedical applications. Biointerface Res Appl Chem. 2021;11(1):8431–8445. https://doi.org/10.33263/BRIAC111.84318445

6. Sudheesh Kumar PT, Lakshmanan VK, Anilkumar TV, Ramya C, Reshmi P, Unnikrishnan AG, et al. Flexible and microporous chitosan hydrogel/nano ZnO composite bandages for wound dressing: In vitro and in vivo evaluation. ACS Appl Mater Interfaces. 2012;4(5):2618–2629. https://doi.org/10.1021/am300292v

7. Balaure PC, Holban AM, Grumezescu AM, Mogoşanu GD, Bălşeanu TA, Stan MS, et al. In vitro and in vivo studies of novel fabricated bioactive dressings based on collagen and zinc oxide 3D scaffolds. Int J Pharm. 2019;557:199–207. https://doi.org/10.1016/j.ijpharm.2018.12.063

8. Kuppusamy P, Yusoff MM, Maniam GP, Govindan N. Biosynthesis of metallic nanoparticles using plant derivatives and their new avenues in pharmacological applications – An updated report. Saudi Pharm J. 2016;24(4):473–484. https://doi.org/10.1016/j.jsps.2014.11.013

9. Shivaji K, Monica ES, Devadoss A, Kirubakaran DD, Dhas CR, Jain SM, et al. Synthesizing green photocatalyst using plant leaf extract for water pollutant treatment. In: Green photocatalysts. Cham: Springer; 2020. p. 25–46. https://doi.org/10.1007/978-3-030-15608-4_2

10. Hasan S. A review on nanoparticles: Their synthesis and types. Res J Recent Sci. 2015;2277:2502.

11. Pandit C, Roy A, Ghotekar S, Khusro A, Islam MN, Emran TB, et al. Biological agents for synthesis of nanoparticles and their applications. J King Saud Univ Sci. 2022;34(3), Art. #101869. https://doi.org/10.1016/j.jksus.2022.101869

12. Luque PA, Soto-Robles CA, Nava O, Gomez-Gutierrez CM, Castro-Beltran A, Garrafa-Galvez HE, et al. Green synthesis of zinc oxide nanoparticles using *Citrus sinensis* extract. J Mater Sci Mater Electron. 2018;29:9764–9770. https://doi.org/10.1007/s10854-018-9015-2

13. Pachaiappan R, Rajendran S, Ramalingam G, Vo DV, Priya PM, Soto-Moscoso M. Green synthesis of zinc oxide nanoparticles by *Justicia adhatoda* leaves and their antimicrobial activity. Chem Eng Technol. 2021;44(3):551–558. https://doi.org/10.1002/ceat.202000470

14. Vijayakumar S, Vaseeharan B, Sudhakaran R, Jeyakandan J, Ramasamy P, Sonawane A, et al. Bioinspired zinc oxide nanoparticles using *Lycopersicon esculentum* for antimicrobial and anticancer applications. J Cluster Sci. 2019;30:1465–1479. https://doi.org/10.1007/s10876-019-01590-z

15. Rao MD, Gautam P. Synthesis and characterization of ZnO nanoflowers using *Chlamydomonas reinhardtii:* A green approach. Environ Prog Sustain Energy. 2016;35(4):1020–1026. https://doi.org/10.1002/ep.12315

16. Thema FT, Manikandan E, Gurib-Fakim A, Maaza M. Single phase bunsenite NiO nanoparticles green synthesis by *Agathosma betulina* natural extract. J Alloys Compd. 2016;657:655–661. https://doi.org/10.1016/j.jallcom.2015.09.227

17. El-Belely EF, Farag MM, Said HA, Amin AS, Azab E, Gobouri AA, et al. Green synthesis of zinc oxide nanoparticles (ZnO-NPs) using *Arthrospira platensis* (Class: Cyanophyceae) and evaluation of their biomedical activities. Nanomaterials. 2021;11(1), Art. #95. https://doi.org/10.3390/nano11010095

18. Abel S, Tesfaye JL, Nagaprasad N, Shanmugam R, Dwarampudi LP, Krishnaraj R. Synthesis and characterization of zinc oxide nanoparticles using moringa leaf extract. J Nanomater. 2021;2021(1), Art. #4525770. https://doi.org/10.1155/2021/4525770

19. Bala Chennaiah M, Kumar KD, Kumar BS, Tanneeru SR. Characterisation of zinc oxide nanoparticles-herbal synthesised coated with *Ocimum tenuiflorum*. Adv Mater Process Technol. 2022;8(suppl2):466–477. https://doi.org/10.1080/2374068X.2021.1934642

20. Mabrouk M, Elkhooly TA, Amer SK. Actinomycete strain type determines the monodispersity and antibacterial properties of biogenically synthesized silver nanoparticles. J Genet Eng Biotechnol. 2021;19(1), Art. #57. https://doi.org/10.1186/s43141-021-00153-y

21. Shrinet K, Singh RK, Chaurasia AK, Tripathi A, Kumar A. Bioactive compounds and their future therapeutic applications. In: Natural bioactive compounds. London: Academic Press; 2021. p. 337–362. https://doi.org/10.1016/B978-0-12-820655-3.00017-3

22. Nduka FO, Onwurah IN, Obeta CJ, Nweze EJ, Nkwocha CC, Ujowundu FN, et al. Effect of nickel oxide nanoparticles on bioethanol production by *Pichia kudriavzveii* IFM 53048 using banana peel waste substrate. Environ Technol. 2024;45(16):3283–3302. https://doi.org/10.1080/09593330.2023.2215450

23. Numbere A, Gbarakoro TN, Eberechukwu MM. Investigation of the use of mangrove and nypa palm parts as tools for remediating polluted soils in the Niger Delta, Nigeria. Int J Plant Soil Sci. 2022;34(19):226–239. https://doi.org/10.9734/ijpss/2022/v34i1931107

24. Goldstein A, Veres P, Burns E, Briggs MS, Hamburg R, Kocevski D, et al. An ordinary short gamma-ray burst with extraordinary implications: Fermi-GBM detection of GRB 170817A. Astrophys J Lett. 2017;848(2), Art. #L14. https://doi.org/10.3847/2041-8213/aa8f41

25. Bunaciu AA, UdriŞTioiu EG, Aboul-Enein HY. X-ray diffraction: Instrumentation and applications. Crit Rev Anal Chem. 2015;45(4):289–299. https://doi.org/10.1080/10408347.2014.949616

26. Bunaciu AA, Aboul-Enein HY, Hoang VD. Vibrational spectroscopy used in polymorphic analysis. TrAC Trends Anal Chem. 2015;69:14–22. https://doi.org/10.1016/j.trac.2015.02.006

27. Imran Din M, Rani A. Recent advances in the synthesis and stabilization of nickel and nickel oxide nanoparticles: A green adeptness. Int J Anal Chem. 2016;2016(1), Art. #3512145. https://doi.org/10.1155/2016/3512145

28. Nwiloh BI, Uwakwe AA, Akaninwor JO. Phytochemical screening and GC-FID analysis of ethanolic extract of root bark of *Salacia nitida* L. Benth. J Med Plants Stud. 2016;4(6):283–287.

29. Ohkawa H, Ohishi N, Yagi K. Assay for lipid peroxides in animal tissues by thiobarbituric acid reaction. Anal Biochem. 1979;95(2):351–358. https://doi.org/10.1016/0003-2697(79)90738-3

30. Singh RP, Chidambara Murthy KN, Jayaprakasha GK. Studies on the antioxidant activity of pomegranate (*Punica granatum*) peel and seed extracts using in vitro models. J Agric Food Chem. 2002;50(1):81–86. https://doi.org/10.1021/jf010865b

31. Pejin B, Bogdanović-Pristov J. ABTS cation scavenging activity and total phenolic content of three moss species. Hem Ind. 2012;66(5):723–726. https://doi.org/10.2298/HEMIND120131022P

32. Jagetia GC, Baliga MS. The evaluation of nitric oxide scavenging activity of certain Indian medicinal plants in vitro: A preliminary study. J Med Food. 2004;7(3):343–348. https://doi.org/10.1089/jmf.2004.7.343

33. Alachaher FZ, Dali S, Dida N, Krouf D. Comparison of phytochemical and antioxidant properties of extracts from flaxseed (*Linum usitatissimum*) using different solvents. Int Food Res J. 2018;25(1):75–82.

34. Kushwaha AS, Kumar A, Kumar R, Srivastava SK. A study of surface plasmon resonance (SPR) based biosensor with improved sensitivity. Photonics Nanostruct Fundam Appl. 2018;31:99–106. https://doi.org/10.1016/j.photonics.2018.06.003

35. Sharmila G, Thirumarimurugan M, Muthukumaran C. Green synthesis of ZnO nanoparticles using *Tecoma castanifolia* leaf extract: Characterization and evaluation of its antioxidant, bactericidal and anticancer activities. Microchem J. 2019;145:578–587. https://doi.org/10.1016/j.microc.2018.11.022

36. Nagarajan S, Arumugam Kuppusamy K. Extracellular synthesis of zinc oxide nanoparticle using seaweeds of gulf of Mannar, India. J Nanobiotechnol. 2013;11, Art. #39. https://doi.org/10.1186/1477-3155-11-39

37. Sutradhar P, Saha M. Green synthesis of zinc oxide nanoparticles using tomato (*Lycopersicon esculentum*) extract and its photovoltaic application. J Exp Nanosci. 2016;11(5):314–327. https://doi.org/10.1080/17458080.2015.1059504

38. Lim YJ, Choi YE, Kang SW, Kim DY, Lee SH, Hahn YB. Vertical alignment of liquid crystals with zinc oxide nanorods. Nanotechnology. 2013;24(34), Art. #345702. https://doi.org/10.1088/0957-4484/24/34/345702

39. Eid MM. Characterization of nanoparticles by FTIR and FTIR-microscopy. In: Mallakpour S, Hussain CM, editors. Handbook of consumer nanoproducts. Singapore: Springer; 2022. p. 1–30. https://doi.org/10.1007/978-981-15-6453-6_89-1

40. Stoia M, Istratie R, Păcurariu C. Investigation of magnetite nanoparticles stability in air by thermal analysis and FTIR spectroscopy. J Therm Anal Calorim. 2016;125:1185–1198. https://doi.org/10.1007/s10973-016-5393-y

41. Akintelu SA, Folorunso AS. A review on green synthesis of zinc oxide nanoparticles using plant extracts and its biomedical applications. BioNanoSci. 2020;10:848–863. https://doi.org/10.1007/s12668-020-00774-6

42. Mirza AU, Kareem A, Nami SA, Bhat SA, Mohammad A, Nishat N. *Malus pumila* and *Juglen regia* plant species mediated zinc oxide nanoparticles: Synthesis, spectral characterization, antioxidant and antibacterial studies. Microb Pathog. 2019;129:233–241. https://doi.org/10.1016/j.micpath.2019.02.020

43. Azizi S, Ahmad MB, Namvar F, Mohamad R. Green biosynthesis and characterization of zinc oxide nanoparticles using brown marine macroalga *Sargassum muticum* aqueous extract. Mater Lett. 2014;116:275–277. https://doi.org/10.1016/j.matlet.2013.11.038

44. Mahendra C, Murali M, Manasa G, Ponnamma P, Abhilash MR, Lakshmeesha TR, et al. Antibacterial and antimitotic potential of bio-fabricated zinc oxide nanoparticles of *Cochlospermum religiosum* (L.). Microb Pathog. 2017;110:620–629. https://doi.org/10.1016/j.micpath.2017.07.051

45. Kumar SS, Venkateswarlu P, Rao VR, Rao GN. Synthesis, characterization and optical properties of zinc oxide nanoparticles. Int Nano Lett. 2013;3(1), Art. #30. https://doi.org/10.1186/2228-5326-3-30

46. Mirza S, Hussaini AA, Öztürk G, Turgut M, Öztürk T, Tugay O, et al. Photocatalytic and antibacterial activities of ZnO nanoparticles synthesized from *Lupinus albus* and *Lupinus pilosus* plant extracts via green synthesis approach. Inorg Chem Commun. 2023;155, Art. #111124. https://doi.org/10.1016/j.inoche.2023.111124

47. Gülçin İ, Şat İG, Beydemir Ş, Elmastaş M, Küfrevioğlu Öİ. Comparison of antioxidant activity of clove (*Eugenia caryophylata* Thunb) buds and lavender (*Lavandula stoechas* L.). Food Chem. 2004;87(3):393–400. https://doi.org/10.1016/j.foodchem.2003.12.008

48. Faisal S, Jan H, Shah SA, Shah S, Khan A, Akbar MT, et al. Green synthesis of zinc oxide (ZnO) nanoparticles using aqueous fruit extracts of *Myristica fragrans*: Their characterizations and biological and environmental applications. ACS Omega. 2021;6(14):9709–9722. https://doi.org/10.1021/acsomega.1c00310

49. Elufioye TO, Unachukwu CC, Oyedeji AO. Anticholinesterase and antioxidant activities of *Spilanthes filicaulis* whole plant extracts for the management of Alzheimer's disease. Curr Enzyme Inhib. 2019;15(2):103–113. https://doi.org/10.2174/1573408015666190730113405

50. Vijayakumar N, Bhuvaneshwari VK, Ayyadurai GK, Jayaprakash R, Gopinath K, Nicoletti M, et al. Green synthesis of zinc oxide nanoparticles using *Anoectochilus elatus*, and their biomedical applications. Saudi J Biol Sci. 2022;29(4):2270–2279. https://doi.org/10.1016/j.sjbs.2021.11.065

51. Kandiah M, Chandrasekaran KN. Green synthesis of silver nanoparticles using *Catharanthus roseus* flower extracts and the determination of their antioxidant, antimicrobial, and photocatalytic activity. J Nanotechnol. 2021; 2021(1), Art. #5512786. https://doi.org/10.1155/2021/5512786